International Journal of Fluid Machinery and Systems
Vol. 2, No. 2, April-June 2009

Original Paper

Experimental Research for Performance and Noise of Small Axial Fan

Takahiro Ito[1], Gaku Minorikawa[2] and Qinyin Fan[3]

[1] Orientalmotor Corporation, 3-4-10 Takarada, Tsuruoka, Yamagata, 997-0011 Japan
[2] Hosei University, 3-7-2 Kajino-cho, Koganei, Tokyo 184-8584 Japan
[3]Jiangsu University, 301 Xuenfu Road, Zhenjiang, Jiangsu, 212013 P.R. China

Abstract

Small axial fans have become widely used as cooling devices in recent years. Because of their increasing importance, studies have been conducted on ways to improve the performance and reduce the noise of such fans. In this report, a small axial fan with a diameter of 85 mm (a type popularity used in personal computer or workstation) was selected for further examination. The influence on aerodynamic performance and noise of such frame design parameters as blade tip clearance results in a decrease of discrete frequency noise and an increase of broad-spectrum noise. As for the most suitable design refinement in terms of fan efficiency, we found that the treatment of outlet corner roundness and altering spoke skew to the direction counter to that of fan rotation was effective.

Keywords: Axial Flow Fan, Performance, Efficiency, Noise, Frame

1. Introduction

Small axial fans have taken an important place in thermal design as the electronic products have become increasingly miniaturized. Concurrently, huge numbers of these inexpensive fans have been produced for use in products such as personal computers. And, while improvements in the mechanical performance of a single small fan would not make much difference in immediate environmental terms, given the immense number of such fans, there are increasing demands from society that designers ensure maximum levels of efficiency.

Several reports have been published about improving the efficiency and reducing the noise from axial fans, but these reports address large fans with diameters of 300 mm or greater. Kamaya et al. examined the characteristics of a small fan with a diameter of 120 mm, but few other researchers have published reports on fans of this size. The objective of the research by Kamaya et al. was reduce the noise emitted by the fan adjusting the clearance between the fan blades and the frame, and the shapes as seen from in front of the fan.

In addition to the shape of the blades, determining the optimum configuration and dimensions of the frame are essential considerations for improving efficiency and reducing the noise of an axial fan. However, due to their low Reynolds number ($Re \approx 10^4$) and the low ratio of blade span to tip clearance, simple copying the designs of larger fans and reducing their dimensions does not always result in the expected levels of performance in smaller fans.

For these and other reasons, small fans are normally designed and improved via the simple “cut-and-try” approach, which is normally expedient since such fans are relatively inexpensive and easy to make.

However, use of such a simple method can do little more than speed up the design of a single fan model. As things currently stand, no parametric rules have yet been established, fan design and production methods remain closely guarded by each manufacturer, and there is little in the way of guidelines or information available for general use.

As a result, there have been few examples of published systematic studies regarding small axial fans and industry is eager for researchers to establish design procedures.

This study addresses the characteristics of the small axial fans with diameter of about 85 mm that are typically used in personal computers and workstations. The objective was to determine ways to increase the efficiency and reduce the noise of these fans. The authors investigated the fan efficiency and noise, as influenced by the frame, changing the blade tip clearance, outlet corner (chamfer width), and varying the angle of the spokes (see Figure 1).

CFD analyses were also performed to investigate what effects flow changes caused by alternations in the frame configuration would have on efficiency and noise.

Received March 3 2009; accepted for publication May 15 2009: Review conducted by Prof. Huang Dian-gui. (Paper number O09002)
Corresponding author: Takahiro Ito, wing@orientalmotor.co.jp

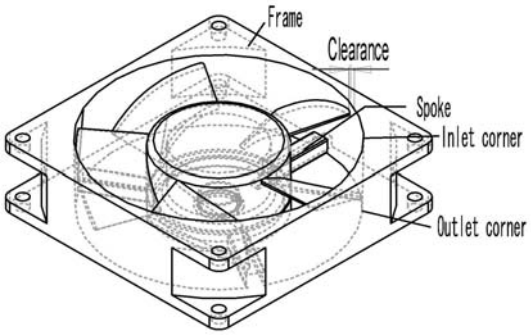

Fig. 1 Schematic view of axial fan

2. Experimental Apparatus and Test Fan

2.1 Experimental apparatus

The flow rate-pressure curve was evaluated in the double-chamber test apparatus shown in Figure 2, which is based on JIS B8330 and AMCA 210-74. The flow rate was calculated from the pressure difference of the venturi nozzles across the test apparatus. The static pressure was measured in the test chambers. The flow rates and pressures found in this test were normalized to the dimensionless flow rate coefficient φ and pressure coefficient ψ as:

$$\phi = Q \Big/ \left[\left(\pi D^2 \Big/ 4 \right) u \right] \quad \cdots(1)$$

$$\psi = 2P_t \Big/ \rho u^2 \quad \cdots(2)$$

Where Q, P_t and ρ presented the flow rate, total pressure and air density, respectively, and D and u represented the fan outer diameter and blade tip circumferential velocity, respectively.

The fan efficiency η was calculated with the following expression:

$$\eta = P_t Q \Big/ T\omega \quad \cdots(3)$$

Where T is the motor torque and ω is the angular velocity of the blade. During the experiment, the angular velocity was constantly measured with a tachometer, but it was difficult to measure the torque of the blade in the fully assembled fan system. Therefore, an identical motor was obtained and tested in a preliminary experiment, and a torque performance curve was taken at the same operating voltage in the experiment of the fully assembled fan. Torque was estimated from the fan rotational velocity in the experiments of the fully assembled fan.

Fan noise was measured in an anechoic chamber as shown in Figure 3, where the test fan was placed 1 m above the floor and rotated at 3,000 rpm. The noise produced was measured with a microphone placed 1 m from the intake. The noise waveform was analyzed with a FFT spectrum analyzer into frequency band components 12.5 Hz in width and A-weighted sound levels were taken.

Noise is dependent on flow rate and the stagnation pressure, so the measured sound pressure level L was converted to the specific sound pressure level L_s in Eq. (4). It was not possible to measure the flow rate or pressure under open flow conditions here, so the maximum airflow rate *Q* detected with the apparatus shown in Figure 2 was used for the standard level.

$$L_s = L - 10 \cdot \log_{10} P_T{}^2 Q \cdots(4)$$

A three-dimensional unsteady flow CFD analysis was also carried out on the commercial unstructured mesh code SCRYU/Tetra in order to examine the relation of internal flow to efficiency and noise. This tool is based on the Navier-Stokes equations. The standard k-ε model of turbulence was used.

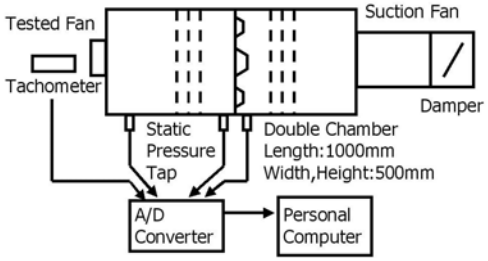

Fig. 2 Experimental apparatus for fan performance

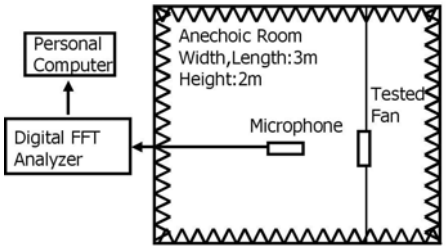

Fig. 3 Experimental apparatus for fan noise

2.2 Test fan

The variable frame parameters on the small axial fan were the blade tip-frame clearance, the outlet shape, and the spoke angle. Fans were fabricated in accordance with the dimensions given in Table 1 and the effects on fan characteristics and noise were observed.

The clearance δ between the blade tip and the frame was varied from 0.5 mm to 2 mm with a constant blade span used (B = 21 mm). As shown in Figure 4, the outlet was varied from a cylindrical to a conic configuration.

Let us state the number of blades as M, the number of spokes as S, and the rotation rate as n; interference noise (tone noise) is generated with the frequency in multiples of MSn. If the number of the sides of the frame is N, an additional tone noise (with the frequency in multiples of MNn) is also generated. When the number of spokes is the same as the number of frame sides, the two-tone noises have identical frequencies and the sources cannot be distinguished. So, the fans in this experiment were designed with three uniformly spaced spokes in order to avoid this issue. The spokes were set an angles from -60° to +60°, in the direction of blade rotation.

Figure 5 shows a typical test fan that could be used for cooling electronic appliance. The fan was 92 mm square and 25.4 mm thick. The fan blade parameters were 6% camber, maximum camber at 50% chord, square with uniform thickness, bent into a constant radius. Figure 6 provides the blade dimensions. Outer diameter of the impeller is 85 mm, and the inner diameter of that is 43 mm. The blade span of the tested fan is 21 mm. Cord length of the blade at the outer diameter is 35 mm and that at the inner is 25 mm. And the shape of the blade seen from front is symmetrical.

We made the tested fan using rapid prototype machine (Stratasys's Dimension). Dimensional tolerance of the tested fan is dependent on the accuracy of the rapid prototype machine. And the accuracy of the machine that made the tested fan is 0.1mm.

Figure 7 shows the shape of the domain and the mesh for CFD. We used the arbitrary Eularian-Lagrangian mesh system, which includes a rotational part (right in the figure) and the stationary part (left in the figure). The two parts are connected with discontinuous meshes.

The CFD model has hemisphere inlet and the cubic outlet. The diameter of the hemisphere inlet is ten times of the diameter of the tested fan impeller. And the cubic outlet has the same dimension to the apparatus of the fan performance. At the surface of the inlet, total pressure is se to the zero, and at the surface of the outlet, flow rate is set to the given condition.

Table 1 Specification of tested fan

Fan No.	Clearance ratio δ /B	Radius of outlet corner Ro[mm]	Angle of spoke β [deg]
1	0.024	43	0
2	0.048	43.5	0
3	0.072	44	0
4	0.096	44.5	0
5	0.048	48.5	0
6	0.048	53.5	0
7	0.048	43.5	−60
8	0.048	43.5	−35
9	0.048	43.5	35
10	0.048	43.5	60

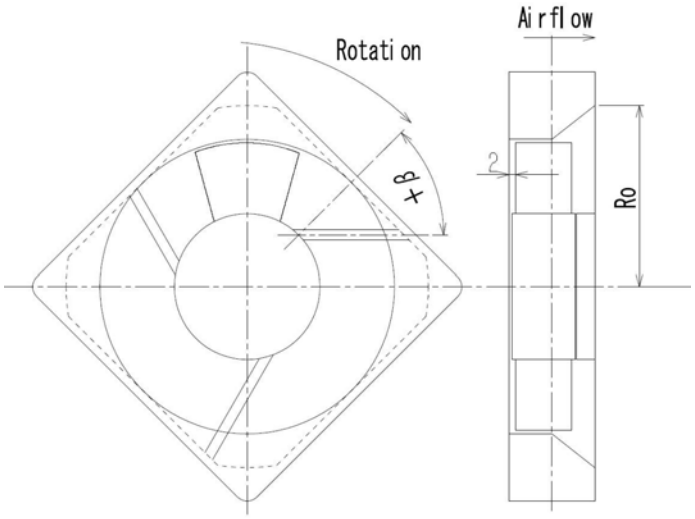

Fig. 4 Configuration of tested frame

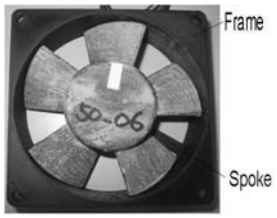

Fig. 5 Configuratin of tested fan

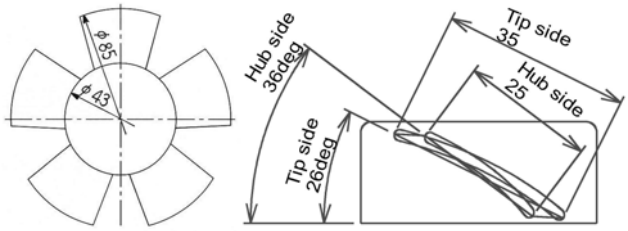

Fig. 6 Profile of wing section

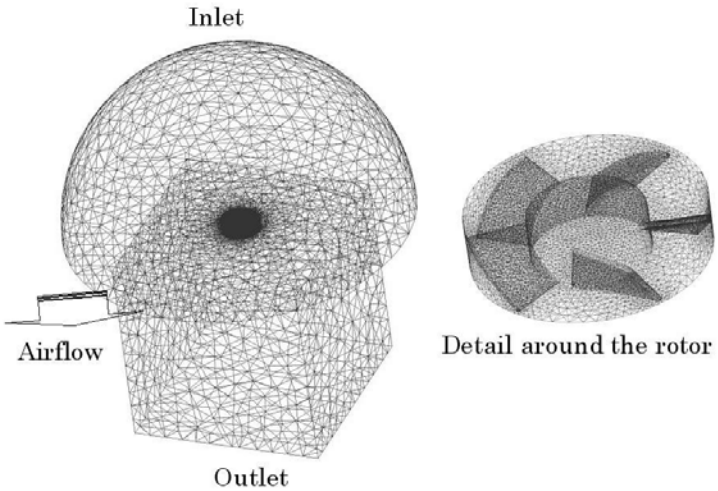

Fig. 7 Domain and the mesh for CFD

3. Experimental Results and Observations

3.1 Effect of blade tip clearance

Figure 8 shows how the flow rate-pressure curves and efficiency changed as a result of varying the blade tip clearance. It is clear that the fan performance and efficiency fell as the clearance increased. Figure 9 presents the efficiency and specific noise as they varied with the ratio of the clearance to the blade span; both of these parameters generally dropped as the clearance increased.

The decrease in efficiency is presumably caused by increasing flow leakage from the pressure side to the suction side of the impeller. No leakage occurs at $\delta = 0$, so that point would be expected to show the efficiency when it is unaffected by clearance. Therefore, the curve was extrapolated to $\delta = 0$ in order to the path to the maximum level of efficiency. Figure 10 shows the relative efficiency η^* curve normalized to the estimated maximum.

The figure predicts that a 1% increase in clearance relative to the blade span results in approximately a 4% cost in efficiency.

Kamaya et al.'s results indicated that noise was increased by widening the clearance, but the present study found just the opposite. Figure 10 shows noise spectra at blade clearance ratios of 0.024 and 0.096, for comparison. It can be seen that with the increase in clearance, discrete frequency components diminished while the broad-spectrum components grew. In other words, the change in the discrete frequency components and in the broad-spectrum components with increase in clearance, showed opposite trends, suggesting differing changes in the noise levels occur with increases in clearance.

Turbulent intensity in the CFD analysis is compared to explain the relationship of the increments of the blade tip clearance and broad-spectrum components. The turbulent model in commercial CFD code used in this research is a Reynolds averaging turbulent model, averaged in space and time. Although it impossible to calculate the broad-spectrum noise directly with the turbulent model, the broad-spectrum noise relates to the turbulent intensity, their variations are compared.

So, we compared the turbulent intensity near the blade tip. To compare the turbulent intensity, we used the result of the CFD. Figure 12 shows the contour map of the turbulent intensity near the blade tip, which was calculated from CFD.

Figure 13 shows the turbulent intensity near the blade tip when the blade clearance ratio is 0.024, and figure 14 shows the turbulent intensity when the blade clearance ratio is 0. 096. It is clear that the turbulent intensity will be large the same as the broad frequency noise, when the blade clearance ratio increases. In other words, the flow leakage at the blade tips increases the turbulent intensity and the broad-spectrum noise the same.

Meanwhile, with the same CFD code, the variations of the discrete frequency components and the variations of the local pressure are evaluated completely.

Figures 15 and 16 show the CFD predicted distributions of pressure and flow vectors over some cross-sections of the test fan, including spokes. In Figure 15, (a) shows the distribution where the maximum pressure is in the vicinity of a spoke, and (b) shows the distribution where the minimum pressure is in the vicinity of the spoke. The blade clearance ratio was 0.024 in Figure 15 and 0.096 in Figure 16.

These Figures indicate that the pressure becomes the maximum in the vicinity of the spoke when the blade passes adjacent to a spoke. As the blade moves and its trailing edge passes the spoke, as shown in Figure 15 (b) and Figure 16 (b), indicated no variation with blade tip clearance and the predicted pressures were nearly identical. In contrast, the maximum pressures in the vicinity of the spoke were higher in the model with a narrower clearance between the blade tip and the frame.

This indicates that the smaller the clearance, the greater the pressure in the vicinity of the spoke, which would be expected to raise discrete frequency component.

Meanwhile, when the pressure in the vicinity of the spoke becomes the maximum, a comparison of the velocity vectors and pressure distributions , in part (a) of Figures 15 and 16 will show that a wider clearance causes back-flow of the air through the gap to the suction side of the blade, thus lowering the pressure in the vicinity of the spoke.

The above results suggest that the back-flow passing through the increasingly wider gap between the blade tip and the frame reduces the pressure on the pressure side of the blade, and reducing efficiency. That is to say, when the blade is directly over the spoke, the pressure near the spoke is also lowered, reducing the pressure fluctuation on the blade, which could be expected to dampen discrete frequency components.

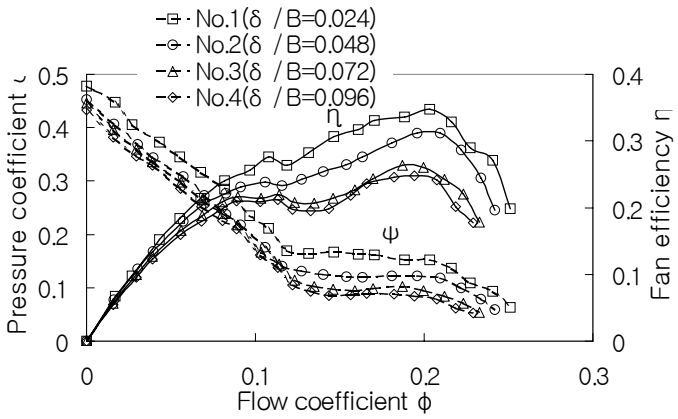

Fig. 8 Performance of characteristics of tested fans (Effects of clearance ratio)

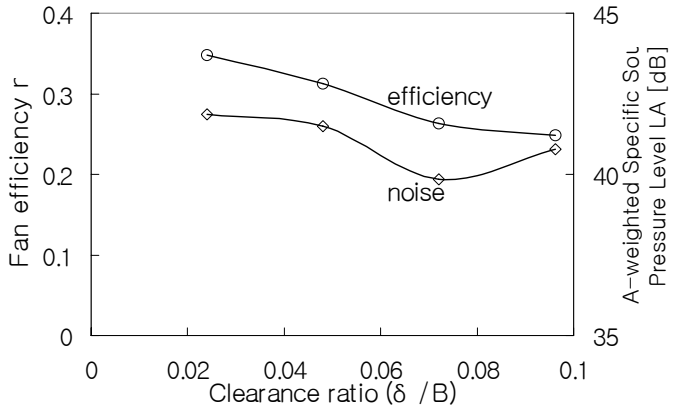

Fig. 9 Effects of clearance ratio

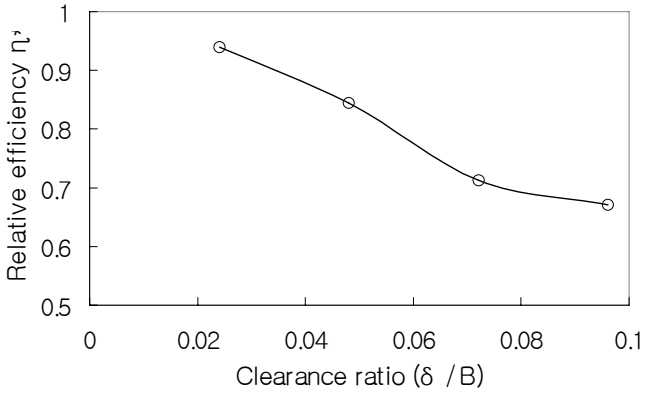

Fig. 10 Effects of clearance ratio

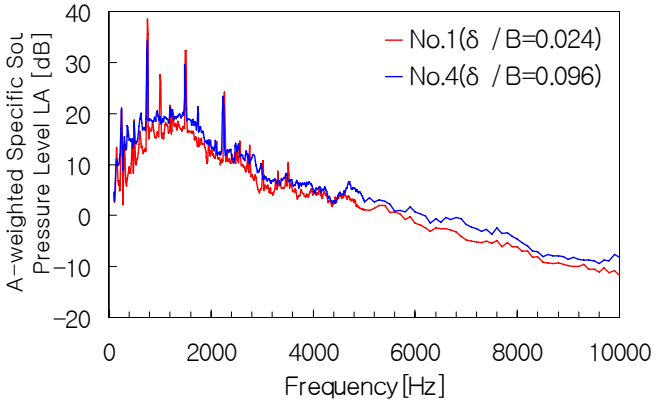

Fig. 11 Noise spectra of tested fans at free air (Effects of clearance ratio)

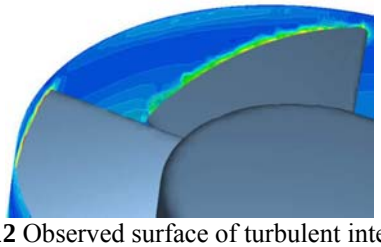

Fig. 12 Observed surface of turbulent intensity

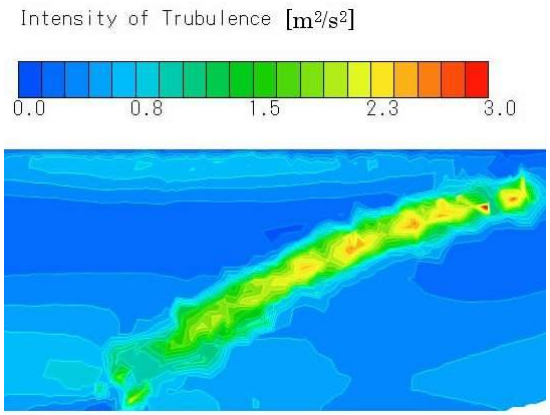

Fig. 13 CFD calculation of turbulent intensity contour of Fan No.1 around the edge of the blade

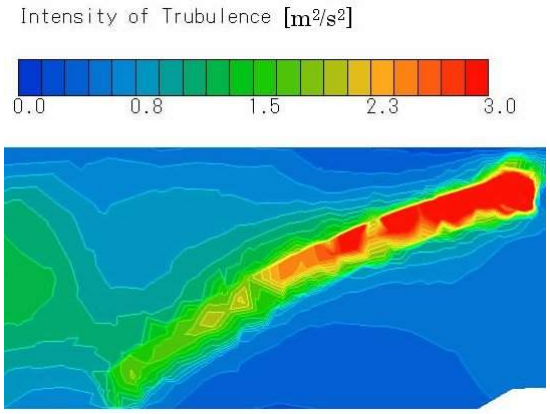

Fig. 14 CFD calculation of turbulent intensity contour of Fan No.4 around the edge of the blade

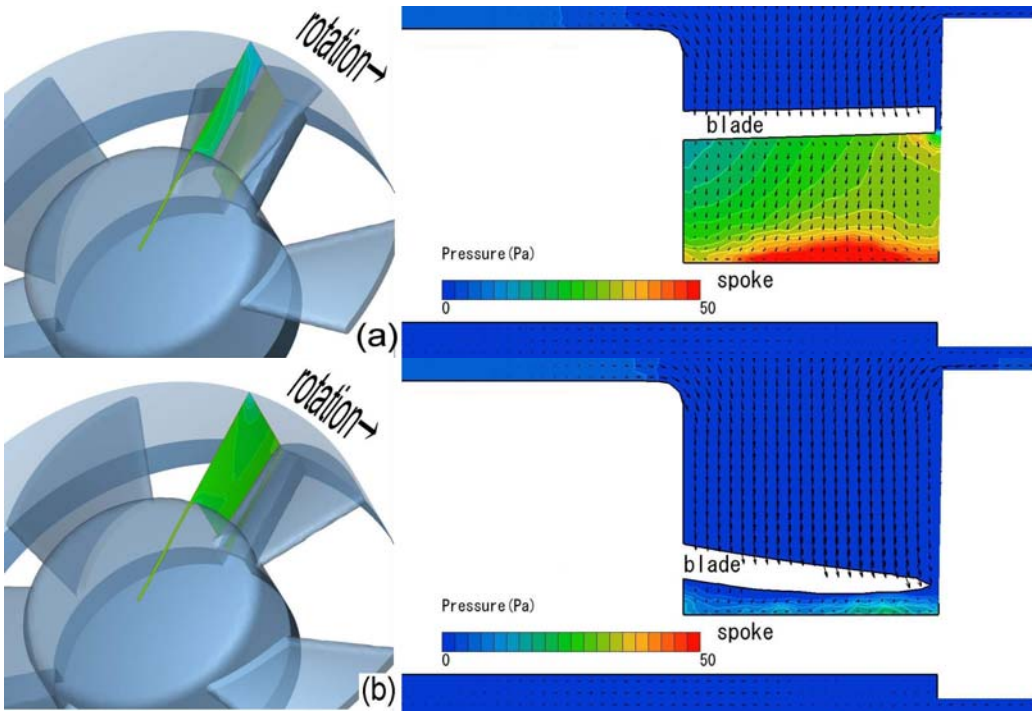

Fig. 15 CFD calculation of pressure contour of Fan No.1 (Clearance ratio is 0.024) at free air (a) pressure around the spoke is maximum and (b) pressure around the spoke is minimum

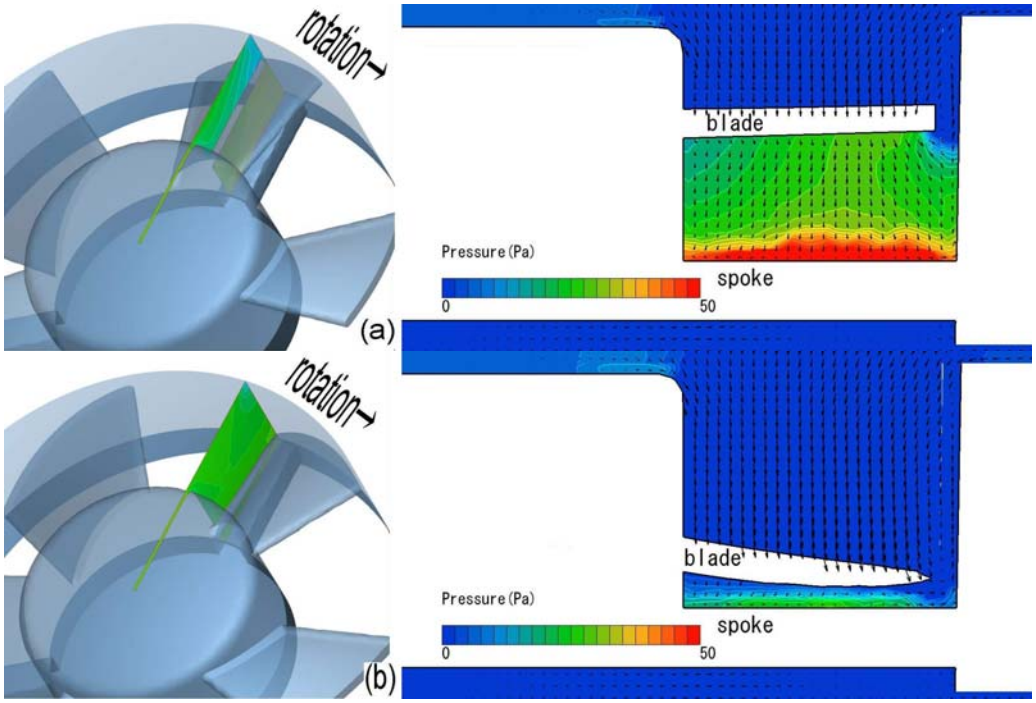

Fig. 16 CFD calculation of pressure contour of Fan No.4 (Clearance ratio is 0.096) at free air (a) pressure around the spoke is maximum and (b) pressure around the spoke is minimum

3.2 Effect of increasing outlet exit radius

Figure 17 shows the curves of flow rate coefficient, pressure coefficient and the efficiency while the chamfer width of the outlet corner was varied.

It can be seen in Figure 17 that increasing this radius improves the fan characteristics and efficiency. This can be attributed to the action of the outlet as a diffuser, transforming the dynamic pressure of the air into static pressure. Figure 18 shows the efficiency as it varies with the ratio of the outlet area to the venturi area. While it can be seen that increasing the chamfer width monotonically improved efficiency, Figure 19 shows, the noise was almost unaffected.

Thus, it is clear that reshaping the outlet into a conic section and increasing its final cross-section area improves fan efficiency.

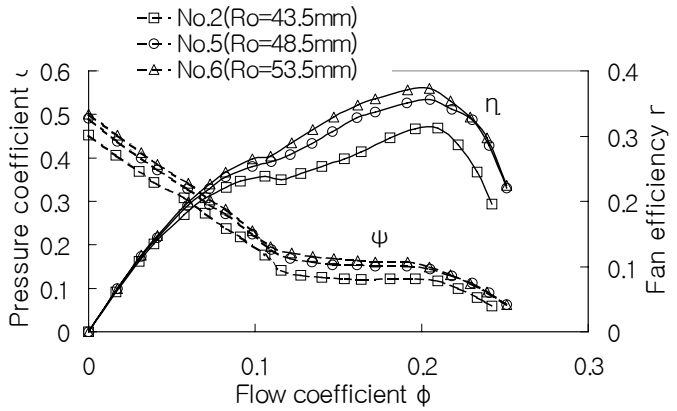

Fig. 17 Performance of characteristics of tested fans (Effects of radius of outlet corner)

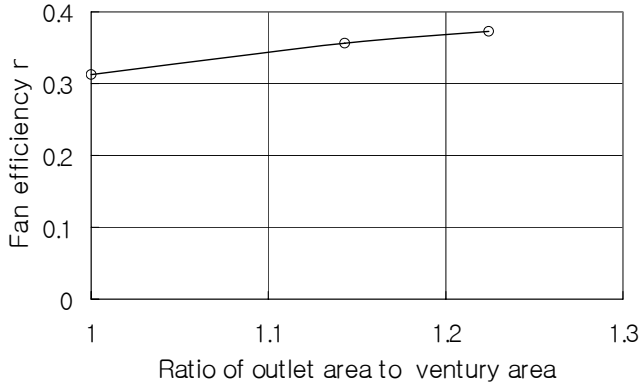

Fig. 18 Effects of outlet area on fan efficiency

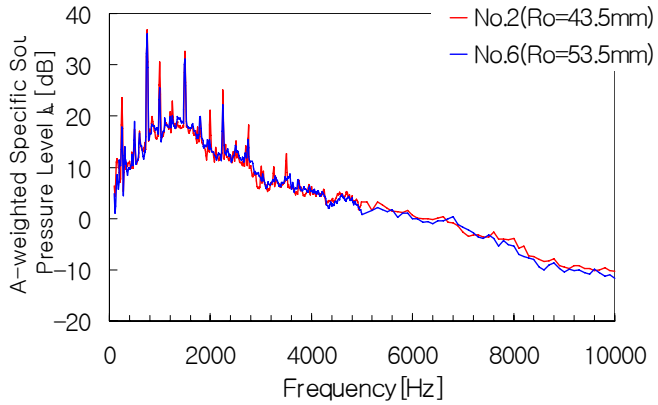

Fig. 19 Noise spectra of tested fans (Effects of radius of outlet corner)

3.3 Effect of spoke angle

Interference noise is caused when the fan blades pass near the spokes. It is already known that this noise can be suppressed by tilting the spokes in order to spoil the simultaneity of the interference. Spokes are normally designed in a slanted pattern for just this reason, but the slant is sometimes in the direction of fan rotation and sometimes in the opposite direction. At the time this study was conducted, it had not been established how the parameters of spoke tilt affect noise. Therefore, we proceeded to vary the tilt while observing fan efficiency and noise.

Figure 20 shows how fan characteristics and efficiency varied with changes to the spoke tilt angle β from -60° to +60°. As shown in the figure, efficiency fell as the spoke was tilted in the positive direction, i.e., as the outer end was shifted circumferentially in the direction of blade rotation.

Now, let us consider the CFD findings in light of the above.

Figures 21 and 22 show the predicted flow vectors and the distribution of the axial component of velocity on a horizontal plane including a spoke.

The flow from the outlet includes vortical components in the direction of blade rotation; these do not contribute to fan output. Figure 21 shows the downstream conditions of a spoke tilted in the rotational direction. It is visible here that the flow colliding with the spoke moves around the spoke in the centrifugal direction and continues downstream with augmented vorticity.

Conversely, when the spokes are tilted opposite to the direction of rotation, the flow colliding with a spoke follows the spoke surface in the centripetal direction (see Figure 22). The pressure is higher in the axial portion of the airway, so the flow along the spoke tends to be swept downstream in the axial direction. As a result, this portion of the vortical components is transformed into axial components, actually augmenting the efficiency of the fan.

Thus, when a spoke is tilted in the counter-rotational direction, it functions as a kind of stator, re-orienting vorticity which otherwise would not contribute to fan output, to the axial direction.

Figure 23 shows the changing of the resulting noise to spoke tilting angles. It is clear that the interference noise induced by the spoke-blade interaction was diminished with spoke tilting, and the 3rd, 6th blade passing frequency components (750Hz, 1500Hz) decreased together. When the spoke was tilted in the rotational direction, the 2nd blade passing frequency (500 Hz) was higher than it was when it was tilted in the counter-rotational direction, but since this blade passing frequency components was generally related to the roundness of the frame, the present finding was considered to be an artifact of inaccuracies in manufacture.

Figure 24 presents the changes in fan efficiency and noise with spoke tilt angle. The frequency components attributed to the spokes decreased as the spokes were tilted, and it is clear that this was not affected by the direction of tilt. Nevertheless, efficiency was higher when the tilt was in the direction opposite to fan rotation.

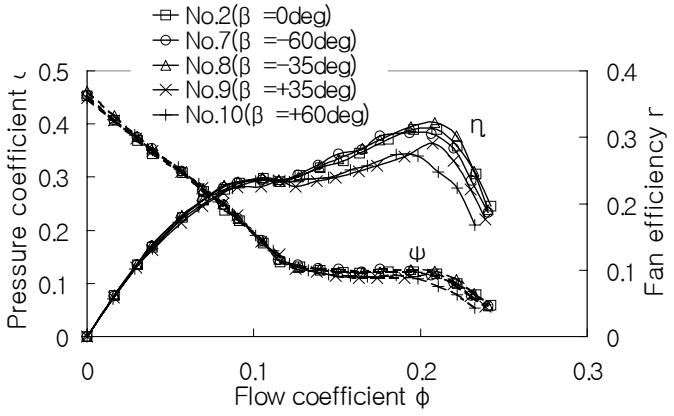

Fig. 20 Performance of characteristics of tested fans (Effects of skew angle of spoke)

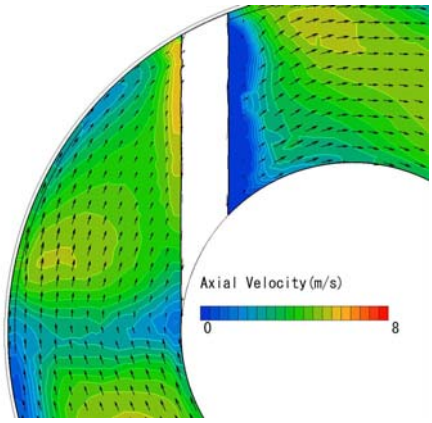

Fig. 21 CFD calculation of flow vector and axial velocity contour of Fan No.10 (Angle of spoke is +60 deg) at maximum efficiency

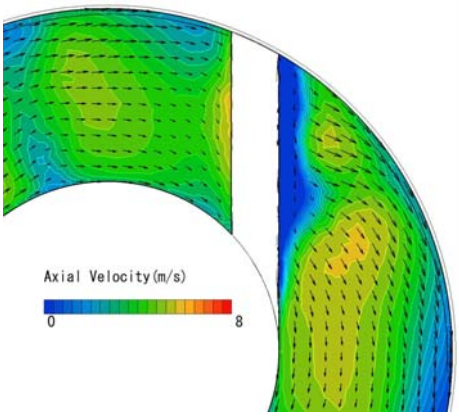

Fig. 22 CFD calculation of flow vector and axial velocity contour of Fan No.7 (Angle of spoke is –60 deg) at maximum efficiency

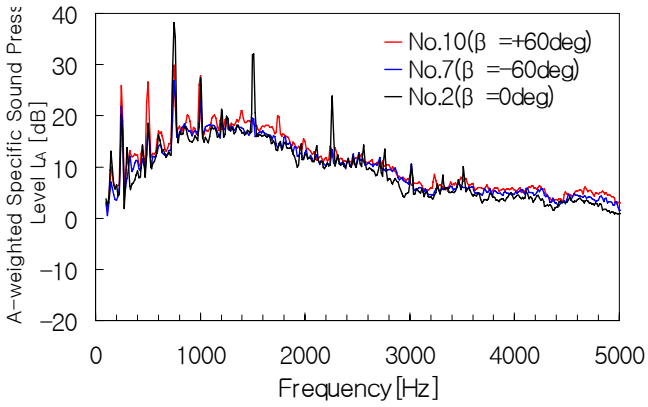

Fig. 23 Noise spectra of tested fans at free air (Effects of rotational skew and counter rotational skew of spoke)

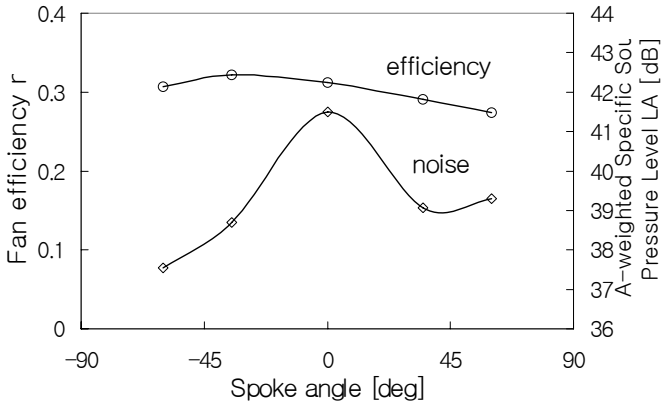

Fig. 24 Effects of skew angle of spoke on fan efficiency and noise

4. Conclusions

The following results were obtained in this investigation into the influences of certain design parameters on the performance and noise of a small axial fan:

1. The efficiency was decreased significantly by increasing the clearance between fan blade tips and frame. In terms of the blade span, a 1% increase of the gap over an initial theoretical gap of zero caused about a 4% decrease in efficiency.
2. Wideband noise components were increased and discrete noise frequency components were decreased by increasing blade clearance.
3. Widening the fan outlet was found to improve efficiency because the widening acted as a diffuser. This did not make any difference in noise production.
4. The efficiency of the fan varied with the tilt of the spokes with respect to the radial direction. Efficiency was increased by tilting the spokes in the counter-rotational direction.
5. Reducing the blade tip clearance, widening the outlet and tilting the spokes in the counter-rotational direction reduced leakage flows, increased the static pressure due to the diffuser effect, and allowed recovery of vortical components, all of which were mutually independent events. The combination of all of these can provide improvements in efficiency. Therefore, an effective method to improve fan efficiency is to make the blade tip clearance as small as possible and within manufacturing tolerances, flaring the outlet into a nozzle shape, and tilting the spokes in the counter-rotational direction.
6. To improve the noise performance of small axial fans, the discrete frequency components should be reduced by tilting the spokes. Reducing the blade tip clearance in order to reduce wideband components was also found to be effective, but this was simultaneously found to increase discrete frequency components. In order to reduce the noise from fans independently of size and other characteristics, it is necessary to identify design factors, which only affect noise. The authors will investigate reshaping the outlet exit to a bell mouth, which appeared only to affect the wideband noise components.

References

[1] Fukano,T., Turbomachinary, Vol. 13, No. 12 (1985), pp. 730-738.
[2] Kozu, T. et al., Turbomachinary, Vol. 32, No. 6 (2004), pp. 343-350.
[3] Kawaguchi, K. et al., Transactions of the Japan Society of Mechanical Engineers, Series B, Vol. 58, No. 554 (1992), pp. 3115-3122.
[4] Kamaya,S. et al.,Transactions of the Japan Society of Mechanical Engineers,Series B, Vol. 56, No. 531 (1990), pp. 3408-3412.
[5] Kondo, H. et al., Turbomachinary, Vol. 19, No. 6 (1991), pp. 333-340.
[6] The Japan Society of Mechanical Engineers ed., JSME Mechanical Engineers' Handbook: Fruids Engineering, pp. 138, The Japan Society of Mechanical Engineers.